

REPORTS

(22). Once a larval stage is reached (day 22), protein metabolism had decreased to 30% of total metabolism (23) and then further declined to 1% for a larva at day 50 (Fig. 3B, right-side of pie chart). At this point in larval development, the sodium pump consumes a very large fraction of total metabolic energy (80%) (10), and a reduction in the cost of protein turnover is necessary to accommodate the sodium pump's demand for cellular energy, given the low metabolic rates of these embryos and larvae.

A relative increase in the rates of mRNA synthesis and protein turnover at -1.5°C is energetically possible in *S. neumayeri*, because the cost of protein metabolism is very low. Indeed, the value we report is lower than has been reported for any other animal. The increase in poly(A⁺) mRNA synthesis can provide a proximate explanation for the unexpectedly high rate of protein turnover in this Antarctic animal. The thermodynamic bases remain to be elucidated for such energy efficiency of protein turnover at low temperatures. Further analyses of the processes underlying the greater energy efficiency in protein metabolism may uncover novel mechanisms of biochemical adaptations and lead to a better understanding of metabolic diversity in organisms inhabiting extreme polar environments.

References and Notes

1. F. M. Shilling, D. T. Manahan, *Biol. Bull.* **187**, 398 (1994).
2. A. Clarke, *Oceanogr. Mar. Biol. Annu. Rev.* **21**, 341 (1983).
3. W. Weiser, *Biol. Rev.* **68**, 1 (1994).
4. H. A. Thieringer, P. G. Jones, M. Inouye, *Bioessays* **20**, 49 (1998).
5. J. R. Welborn, D. T. Manahan, *J. Exp. Biol.* **198**, 1791 (1995).
6. Early work on protein synthesis rates in sea urchin embryos has demonstrated a rapid equilibration between the intracellular free amino acid pool and the charged tRNA pool (24).
7. Amino acid composition of proteins was examined during development in *S. neumayeri* by gas-phase acid hydrolysis and high-performance liquid chromatography quantification of constituent amino acids (5, 25). A trichloroacetic acid precipitation step was used to isolate protein from whole embryos and larvae for the analyses. Seven different developmental time points were measured between fertilization and the first larval stage (day 22).
8. Respiration rates were measured using 1-ml glass respiration vials for end-point measurements of oxygen tension using a polarographic oxygen sensor (26, 27). Six vials with 50 to 200 embryos or larvae were measured at each experimental point by sealing the vials and incubating them for 8 hours at -1.5°C . Oxygen tension was then measured by injecting 500 μl of the seawater from a vial into a 50- μl microcell maintained at -1.5°C . This technique was specifically optimized for use with *S. neumayeri* embryos and larvae and cross-checked with four other independent methods for measuring oxygen consumption rates.
9. Protein synthesis rates were measured during 90-min time-course experiments of radiolabel incorporation into trichloroacetic acid-precipitable protein (28). During embryogenesis, rates were measured on four separate cultures (started from different parents at different times), and two of these were further used for studies during later larval development. In all experiments, 12,000 individuals were placed in 12 ml of sterile filtered seawater (0.2 μm) with 70 μCi of [¹⁴C]alanine. Individuals were incubated at -1.5°C

- with the radiolabel, and 500- μl aliquots were removed at 15-min intervals for measurements of both the protein incorporation and the specific activity of [¹⁴C]alanine in the free amino acid pool. Corroborative measurements were also made using [¹⁴C]leucine.
10. P. K. K. Leong, D. T. Manahan, *J. Exp. Biol.* **202**, 2051 (1999).
11. The number of cells in the blastulae stage has been measured previously, 2152 cells (27), allowing a calculation here of a cell-specific rate of protein synthesis of 1.49 pg protein per hour per cell.
12. A. S. Goustin, F. H. Wilt, *Dev. Biol.* **82**, 32 (1981).
13. W. E. Berg, D. H. Mertes, *Exp. Cell Res.* **60**, 218 (1970).
14. B. J. Fry, P. R. Gross, *Dev. Biol.* **21**, 125 (1970).
15. E. H. Davidson, *Gene Activity in Early Development* (Academic Press, Orlando, FL, ed. 3, 1986).
16. R. S. Wu, F. H. Wilt, *Dev. Biol.* **41**, 352 (1974).
17. M. Ito, J. Bell, G. Lyons, R. Maxson, *Dev. Biol.* **129**, 147 (1988).
18. D. F. Houlihan, in *Advances in Comparative and Environmental Physiology*, R. Gilles, Ed. (Springer-Verlag, Berlin, 1991), vol. 7, pp. 1–43.
19. A. J. Hawkins, J. Widdows, B. L. Bayne, *Physiol. Zool.* **62**, 745 (1989).

20. A. R. Lyndon, D. F. Houlihan, S. J. Hall, *Arch. Int. Physiol. Biochem.* **97**, C31 (1989).
21. P. J. Reeds, *Anim. Prod.* **45**, 149 (1987).
22. W. G. Siems, H. Schmidt, S. Gruner, M. Jakstadt, *Cell Biochem. Funct.* **10**, 61 (1992).
23. A. G. Marsh, R. E. Maxson Jr., D. T. Manahan, data not shown.
24. J. C. Reiger, F. C. Kafatos, *Dev. Biol.* **57**, 270 (1977).
25. R. Henrikson, S. Meredith, *Anal. Biochem.* **136**, 65 (1984).
26. A. G. Marsh, D. T. Manahan, *Mar. Ecol. Prog. Ser.* **184**, 1 (1999).
27. A. G. Marsh, P. K. K. Leong, D. T. Manahan, *J. Exp. Biol.* **202**, 2041 (1999).
28. J. Vavra, D. T. Manahan, *Biol. Bull.* **196**, 177 (1999).
29. This work was supported by the National Science Foundation OPP-9420803. We thank T. Hamilton for technical assistance with the experiments and chromatographic analyses. This paper is dedicated to the late Catherine Manahan.

4 October 2000; accepted 30 January 2001

Published online 15 February 2001;

10.1126/science.1056341

Include this information when citing this paper.

A Short Duration of the Cretaceous-Tertiary Boundary Event: Evidence from Extraterrestrial Helium-3

S. Mukhopadhyay,^{1*} K. A. Farley,¹ A. Montanari²

Analyses of marine carbonates through the interval 63.9 to 65.4 million years ago indicate a near-constant flux of extraterrestrial helium-3, a tracer of the accretion rate of interplanetary dust to Earth. This observation indicates that the bolide associated with the Cretaceous-Tertiary (K-T) extinction event was not accompanied by enhanced solar system dustiness and so could not have been a member of a comet shower. The use of helium-3 as a constant-flux proxy of sedimentation rate implies deposition of the K-T boundary clay in $(10 \pm 2) \times 10^3$ years, precluding the possibility of a long hiatus at the boundary and requiring extremely rapid faunal turnover.

The K-T boundary at 65 million years ago (Ma) records a major mass-extinction event and, though the occurrence of an extraterrestrial impact (1, 2) is widely accepted, the nature of the impactor and its role in the K-T mass extinction is debated. Possible candidates for the impactor are a single asteroid or comet (1–3) or a member of a comet shower (4). An extraterrestrial impact would have severely perturbed Earth's ecosystems and climate by injecting large quantities of dust (1) and climatically active gases (5) into the atmosphere. An alternative hypothesis to explain the biotic calamity invokes voluminous volcanism (6). Recent work (7) suggests that

most of the Deccan Traps flood basalts were erupted in a <1-million-year (My) interval coincident with the K-T boundary. The global environmental effects from extensive volcanism could be similar to the effects from a large impact (6), but the time scale of the two processes would be different. The perturbation on climate and ecosystems from an impact would be geologically instantaneous, but the effects from volcanism would be spread over at least a few hundred thousand years.

The K-T boundary clay is a distinctive bed, typically a few cm thick, that separates sedimentary rocks of the Cretaceous from those of the Tertiary. Knowledge of the deposition interval of the clay would provide important insights into the cause(s) and rates of mass extinction and climate change at the boundary, but most geochronologic tools are inadequate for this purpose. Estimates of this time interval are based on the assumption that the K-T clay was deposited at the same rate

¹Division of Geological and Planetary Sciences, California Institute of Technology, Pasadena, CA 91125, USA. ²Osservatorio Geologico di Coldigioco, 62020 Frontale di Apiro, Italy.

*To whom correspondence should be addressed. E-mail: sujoy@gps.caltech.edu

REPORTS

as the clay fraction in the surrounding paleomagnetically dated limestones [e.g., (8)]; this assumption is questionable during such a turbulent period. Cyclostratigraphy constrains the sedimentation rate before and after the K-T boundary (9), but cannot be applied to the clay itself. The duration of the K-T boundary is thus uncertain, with estimates ranging from a few thousand to hundreds of thousands of years (8–11). Here we use extraterrestrial He to better characterize the K-T impactor and the depositional interval of the associated clay.

Accumulation of interplanetary dust particles (IDPs) imparts high ^3He concentrations ($[\text{He}]_{\text{Et}}$) and high $^3\text{He}/^4\text{He}$ ratios to many deep-sea sediments (12). Extraterrestrial materials have higher $^3\text{He}/^4\text{He}$ ratios than terrestrial matter ($>100 R_A$ versus $<0.03 R_A$, where R_A is the $^3\text{He}/^4\text{He}$ ratio normalized to the atmospheric value of 1.39×10^{-6}), and this distinction can be used to establish the concentration of extraterrestrial ^3He ($[\text{He}]_{\text{Et}}$) in sedimentary rocks. $[\text{He}]_{\text{Et}}$ is most sensitive to the accretion of IDPs smaller than $\sim 35 \mu\text{m}$ because larger IDPs undergo frictional heating and He loss during atmospheric entry (13). Like large IDPs, large bolides (km sized) should not contribute ^3He -bearing particles to sediments because they are vaporized upon impact; we verify this expectation below. Therefore, unlike platinum-group elements (e.g., Ir and Os), ^3He does not directly record the accretion of single large impactors.

$[\text{He}]_{\text{Et}}$ is described by the relation $[\text{He}]_{\text{Et}} = f_{\text{He}} r / \alpha$, where f_{He} is the extraterrestrial ^3He accretion rate, α is the sediment mass-accumulation rate (MAR), and r is a retentivity parameter that accommodates diagenetic and/or diffusional He losses, varying between unity and zero. Because $[\text{He}]_{\text{Et}}$ is retained in the sedimentary record for at least 480 My (14), we assume a constant r over the few million years of interest for the present problem. Measurements of $[\text{He}]_{\text{Et}}$ in a sedimentary sequence thus constrain the ratio f_{He}/α through time. If f_{He} is constant, this ratio is inversely proportional to the MAR and permits estimation of the instantaneous sedimentation rate without knowledge of absolute age.

We measured He concentration and isotopic ratio on samples from the Gubbio and Monte Conero sections in the Umbrian Apennines of Italy (15) and at three stratigraphic levels in the 0.5-m-thick K-T clay from the Ain Settara section (STW) near El Kef, Tunisia (Table 1) (16, 17). $^3\text{He}/^4\text{He}$ ratios in the Gubbio sediments vary from 1.9 to 0.3 R_A (15) and can be modeled as a two-component mixture of crustal and extraterrestrial He (18). Assuming reasonable end-member $^3\text{He}/^4\text{He}$ ratios of 0.03 R_A

and 290 R_A (19, 20) for the crustal and extraterrestrial components, the calculated $[\text{He}]_{\text{Et}}$ is $>86\%$ of the total ^3He . Helium-4 ($[\text{He}]_{\text{C}}$) is $>99\%$ terrestrial and may therefore be used as a tracer of the relative terrigenous flux (21).

High-frequency scatter in $[\text{He}]_{\text{Et}}$ (Fig. 1A) is probably a statistical artifact of the small number of IDPs hosted in the sediments [e.g., (13)]. A three-point running mean through the data reduces this scatter; the smoothed $[\text{He}]_{\text{Et}}$ is constant to within $\pm 20\%$ from 345 m to the K-T boundary at 347.63 m, increases in the K-T clay, and returns to pre-K-T values within the first limestones of the Tertiary. About 0.5 m above the K-T boundary, $[\text{He}]_{\text{Et}}$ increases briefly, then decreases (Fig. 1).

$[\text{He}]_{\text{Et}}$ is correlated with proxies of relative sedimentation rate (18, 21, 22) such

as sediment noncarbonate fraction (NCF) and $[\text{He}]_{\text{C}}$ (Fig. 1). This correlation implies that between 63.9 and 65.4 Ma, the ^3He accretion rate was constant and $[\text{He}]_{\text{Et}}$ in the sediments was controlled predominantly by changes in carbonate MAR. Hence, the K-T impact was not preceded nor immediately followed by a change in ^3He accretion $>\pm 20\%$. $^3\text{He}/^4\text{He}$ ratio is constant across the K-T boundary (15) (Table 1), and because ^4He and NCF increase when sediment MAR decreases (18, 21, 22), the higher $[\text{He}]_{\text{Et}}$ in the K-T clay is attributable solely to a decrease in sedimentation rate.

Possible candidates for the K-T impactor include an asteroid or comet (1–3), or a member of a shower of long-period comets (4). Showers of long-period comets are produced by gravitational perturbations of

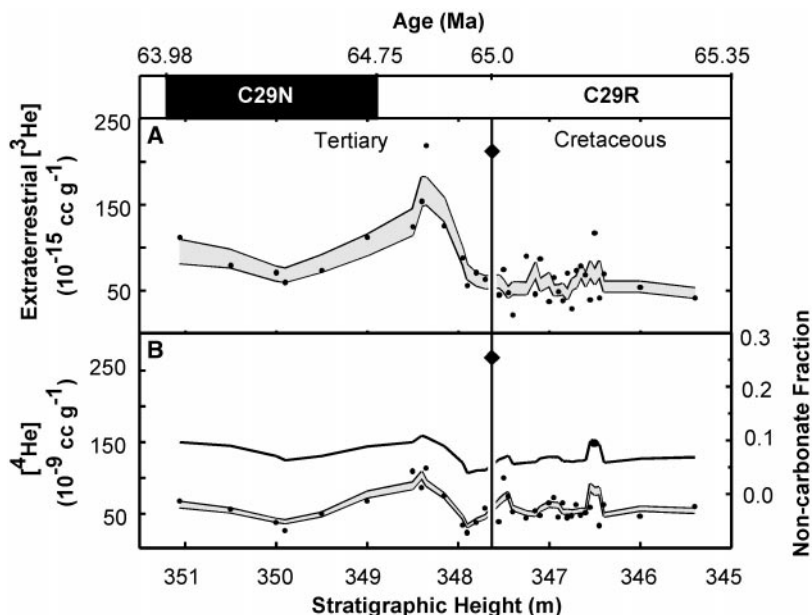


Fig. 1. (A) $[\text{He}]_{\text{Et}}$, (B) $[\text{He}]_{\text{C}}$, and noncarbonate fraction (solid black line) in the Gubbio sediments. Points are individual values and are averages of leached replicates (if replicated). (◆) indicates the K-T boundary clay. He concentrations are per gram of bulk sediment. The shaded envelope represents the 1σ uncertainty of the three-point running mean calculated from the uncertainties of individual data points (18). The K-T boundary sample was not included in the running mean. C29N and C29R refer to magnetic polarity chrons, and the chron boundary ages are from (33).

Table 1. ^3He , ^4He , and $^3\text{He}/^4\text{He}$ ratios in K-T boundary clays. For the Gubbio and Monte Conero K-T clay, an entire strip of the clay was sampled and homogenized before He measurements (15). The reported values therefore represent an average value for the K-T clay. The numbers (in mm) next to the STW site represent the stratigraphic height from the base of the 0.5-m-thick K-T clay layer (16, 17).

Site	$[\text{He}]_{\text{Et}}$ (10^{-15} cm^3 STP g^{-1})	$\pm 1\sigma$	$[\text{He}]_{\text{C}}$ (10^{-9} cm^3 STP g^{-1})	$\pm 1\sigma$	$^3\text{He}/^4\text{He}$ (R_A)
Gubbio	219	25.3	265.7	13.4	0.6
Monte Conero	309	43.7	477.2	67.5	0.5
STW					
0	15	3.0	251.8	50.4	0.04
20	19.9	3.9	551.0	110.0	0.03
80	25.9	5.2	458.5	91.7	0.04

REPORTS

the Oort cloud that enhance the cometary flux over a 1- to 2-My period (4). Cometary activity increases the interplanetary dust abundance in the inner solar system (23), and because this dust is swept into the sun on a lifetime that is shorter than the mean life of a long-period comet (600 ky) (24), terrestrial impacts produced by members of a comet shower should be associated with enhanced IDP (and $^3\text{He}_{\text{Et}}$) accretion (22). The near-constant ^3He accretion rate observed from 65.4 to 63.9 Ma rules out such an event at the K-T boundary. Instead, our data are more consistent with an impact of an asteroid or a lone comet, because a single comet would not markedly increase the total IDP flux. Major collisions in the asteroid belt also enhance the terrestrial accretion rate of IDPs over a 10^4 - to 10^6 -year period (19, 25). Such collisions might lead to new Earth-crossing asteroids in 10^6 years (25), so an increase in inner-solar system dustiness may be associated with an enhanced probability of terrestrial impact. Our $^3\text{He}_{\text{Et}}$ data argue against this scenario for the K-T impactor.

The near-constant ^3He accretion rate across the K-T boundary allows the $^3\text{He}_{\text{Et}}$ record to be inverted for instantaneous sedimentation rate within the K-T clay. In calculating the time associated with the K-T boundary event, we assume that no part of the K-T clay has been lost by erosion or slumping. To test this as-

sumption, we analyzed K-T boundary clays from multiple locations.

Calculated sedimentation rates of the K-T clay vary from 2.5 mm ky^{-1} at Gubbio to 53 mm ky^{-1} at STW (Table 2) (15). The original thickness and density of the K-T boundary clay at Gubbio are uncertain, owing to the presence of secondary calcite (10). The thickness (20 mm) and dry bulk density (2 g cm^{-3}) of the clay at Monte Conero are known with more certainty and are more representative (10). Using these values for the Italian sites, we calculate that the depositional intervals for the K-T clay are $7.9 \pm 1.0 \text{ ky}$ and $10.9 \pm 1.6 \text{ ky}$ at Gubbio and Monte Conero, respectively (Table 2). The deposition interval of the 0.5-m-thick boundary clay at STW is $11.3 \pm 2.3 \text{ ky}$ (Table 2) (26), consistent with the results from the Italian sections. At STW, an ~ 3 -mm-thick layer near the base of the K-T clay has been identified as the fallout lamina (17, 27). On the basis of $^3\text{He}_{\text{Et}}$ measurements, an upper limit for the depositional interval of this layer is $60 \pm 12 \text{ years}$ (Table 2).

The recent discovery of fullerene-hosted extraterrestrial ^3He in K-T boundary clays (28) introduces a potential complication into our calculation. However, the total ^3He contribution from the bolide cannot exceed 8% of the $^3\text{He}_{\text{Et}}$ in the K-T clay from Gubbio (29). Note that if a part of the $^3\text{He}_{\text{Et}}$ is indeed from the bolide, the fraction from

IDPs is lowered, so our computed durations of the boundary event are firm upper limits.

Some investigators [e.g., (11)] have proposed that the mass extinction at the K-T boundary was not catastrophic, but only appears so because of long-duration (100 ky) hiatus(es) at the K-T boundary in many deep-sea sections. A long hiatus in the Gubbio and Monte Conero sites would have resulted in high concentrations of IDPs and consequently a low $^3\text{He}_{\text{Et}}$ -based sedimentation rate. Because our samples from these sites are homogenized strips covering the entire length of the K-T boundary clay, any hiatus present would have been sampled. The computed depositional time of $\sim 10 \text{ ky}$ for the boundary clay, coupled with the agreement from the three different K-T sites, leads us to conclude that there was no long-duration hiatus. The mass extinction at the K-T boundary was an extremely rapid catastrophe, and the time span is too short to be explained by Deccan volcanism, which was erupted over a period $>500 \text{ ky}$ (6, 7). We conclude that the impact of an asteroid or a single comet at the K-T boundary was the main driving force of the biotic calamity.

After the K-T impact, oceanic productivity was drastically reduced (30). Global darkness would have lasted at most a few years, and once surface irradiance returned, it would have been difficult to maintain low-productivity oceans (31). Our data indicate that, in the deep ocean, carbonate sedimentation remained low for the $\sim 10 \text{ ky}$ of K-T clay deposition and, unexpectedly, imply that sedimentation rates after the K-T boundary event returned to and remained constant at pre-K-T values for the next $\sim 20 \text{ ky}$ (Fig. 2). We hypothesize that 10 ky was the time required to restore food chains and repair ecosystems. Subsequently, life rebounded, and the oceans were repopulated with planktonic species characterized by high turnover rates. The initial fauna was then replaced by a more stable fauna with lower turnover rates (32), possibly explaining the drop in sedimentation rate in the early Tertiary. Our reconstruction of the sedimentation history at Gubbio in the Late Cretaceous suggests rapid variations in sedimentation rates on time scales of 10 to 20 ky (Fig. 2), similar to inferences drawn from other sites on the basis of cyclostratigraphy (9). These variations may reflect sedimentation responses to orbital forcing (9) or fluctuations in primary productivity.

Fig. 2. $^3\text{He}_{\text{Et}}$ -based sedimentation rate. Points are values of the instantaneous sedimentation rate; (◆) indicates the K-T boundary. The line is a three-point running mean. A ^3He accretion rate of $106 \times 10^{-15} \text{ cm}^3 \text{ cm}^{-2} \text{ ky}^{-1}$ and a density of 2.7 g cm^{-3} for the limestones as measured by (18) were used to compute sedimentation rates. The arrow indicates an off-scale point. The K-T sample along with the off-scale point were not included in the running mean. Time relative to the K-T boundary was calculated from the ^3He -based sedimentation rate.

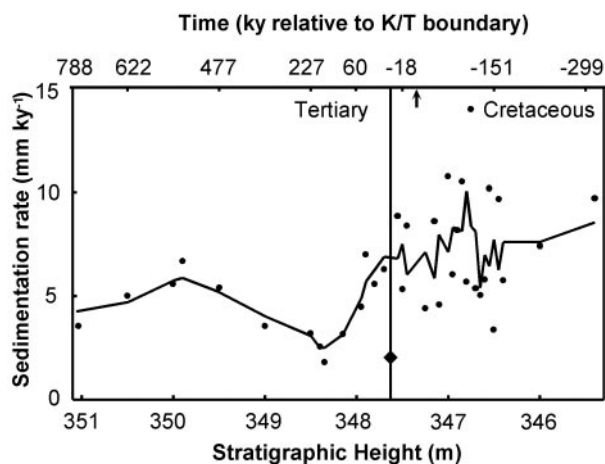


Table 2. Duration of the K-T boundary event. Sedimentation rate was computed with an average ^3He accretion rate of $(106 \pm 4.6) \times 10^{-15} \text{ cm}^3 \text{ cm}^{-2} \text{ ky}^{-1}$ and a density of 2 g cm^{-3} for the boundary clay. The 1σ uncertainty in the duration of the boundary event is the propagated uncertainty of the ^3He accretion rate and measured $^3\text{He}_{\text{Et}}$ (13, 18).

Site	Thickness of K-T clay (mm)	Sedimentation rate (mm ky^{-1})	$\pm 1\sigma$	Duration (ky)	$\pm 1\sigma$
Gubbio	20	2.5	0.3	7.9	1.0
Monte Conero	20	1.8	0.3	10.9	1.6
STW	500	44	9	11.3	2.3
STW Ir-rich layer	3	53	11	<0.06	0.012

References and Notes

1. L. W. Alvarez, W. Alvarez, F. Asaro, H. V. Michel, *Science* **208**, 1097 (1980).
2. A. Shukolyukov, G. W. Lugmair, *Science* **282**, 927 (1998).
3. F. T. Kyte, *Nature* **396**, 237 (1998).
4. P. Hut et al., *Nature* **329**, 118 (1987).

Continuous Mantle Melt Supply Beneath an Overlapping Spreading Center on the East Pacific Rise

Robert A. Dunn,^{1,2*} Douglas R. Toomey,¹ Robert S. Detrick,³
William S. D. Wilcock⁴

Tomographic images of upper mantle velocity structure beneath an overlapping spreading center (OSC) on the East Pacific Rise indicate that this ridge axis discontinuity is underlain by a continuous region of low *P*-wave velocities. The anomalous structure can be explained by an approximately 16-kilometer-wide region of high temperatures and melt fractions of a few percent by volume. Our results show that OSCs are not necessarily associated with a discontinuity in melt supply and that both OSC limbs are supplied with melt from a mantle source located beneath the OSC. We conclude that tectonic segmentation of the ridge by OSCs is not the direct result of magmatic segmentation at mantle depths.

The discovery that fast-spreading oceanic ridges are structurally (1, 2) and chemically (3, 4) segmented between transform offsets has led to competing hypotheses for the origin of ridge segmentation (5, 6). Central to this controversy is the question of the cause of OSCs. OSCs are segment boundaries characterized by the overlap of two ridge segments which offset the axial neovolcanic zone by 0.5 to 15 km. The larger OSCs consist of two distinct ridge limbs that surround a central basin (7). Unlike transform offsets, which are stationary with respect to the ridge, OSCs migrate along axis and, in doing so, individual limbs may propagate, recede, or be rafted off to the side of the rise, leaving behind a distinctive seafloor morphology and disrupted magnetic lineations (7–9). Studies of the wakes of OSCs indicate that these ridge discontinuities are unstable on a time scale as short as 50,000 years (8, 9). The structural evolution of OSCs has led some to speculate that their origin is the result of fluctuations in axial magmatic processes (7, 10). By this view, OSCs occur above regions of reduced magma supply, perhaps at the boundary between two widely separated regions of mantle upwelling (11). This model asserts that OSCs are the result of converging, but

misaligned episodes of lateral (along the ridge axis) magma injection, such that each limb has a separate source of mantle-derived magma. In contrast, an opposing model states that OSCs are the result of tectonic processes, such as those resulting from changes in the kinematics of spreading (1, 12). In this hypothesis, mantle upwelling is approximately two-dimensional or sheet-like, and the magma supply beneath the OSC is uninterrupted. Thus, the morphologically distinct limbs of an OSC share a common source of magma (1).

To test these competing models of magma supply to fast-spreading ridges, we conducted a seismic experiment along the East Pacific Rise (EPR) between the Clipperton and Siqueiros transforms (Fig. 1). Here, we report on a subset of the data which allows imaging of lateral variations in shallow mantle *P*-wave velocity structure beneath an 80-km-long section of the rise that includes the 9°03'N OSC. This OSC and associated ridge segments have been well studied by geophysical mapping (8, 9, 13, 14), petrologic and geochemical analysis of seafloor basalts (3), and multichannel seismic (MCS) experiments (15–17). The OSC consists of two north-south trending ridge segments that overlap by 27 km, are offset by 8 km, and enclose a central basin. In general, normal (N-type) mid-ocean ridge basalts (MORBs) have been recovered from the northern segment of the rise, and enriched-type MORBs have been recovered from the southern segment (3), leading some to infer that this ridge discontinuity separates two physically and chemically distinct sources of magma.

The seismic experiment consisted of an array of 15 ocean-bottom instruments that

5. D. A. Kring, *GSA Today* **8**, 2 (2000).
6. C. B. Officer, A. Hallam, C. L. Drake, J. D. Devine, *Nature* **326**, 143 (1987).
7. C. Hofmann, G. Feraud, V. Courtillot, *Earth Planet. Sci. Lett.* **180**, 13 (2000).
8. J. Smit, A. J. T. Romein, *Earth Planet. Sci. Lett.* **74**, 155 (1985).
9. T. D. Herbert, S. D'Hondt, *Earth Planet. Sci. Lett.* **99**, 263, (1990).
10. A. Montanari, *J. Sed. Petrol.* **61**, 315 (1991).
11. G. Keller, B. Barrera, B. Schmitz, E. Mattson, *Geol. Soc. Am. Bull.* **105**, 979 (1993).
12. M. Ozima, M. Takayanagi, S. Zashu, S. Amari, *Nature* **311**, 449 (1984).
13. K. A. Farley, S. G. Love, D. B. Patterson, *Geochim. Cosmochim. Acta* **61**, 2309 (1997).
14. D. B. Patterson, K. A. Farley, B. Schmitz, *Earth Planet. Sci. Lett.* **163**, 315 (1998).
15. Supplementary data are available on Science Online at www.sciencemag.org/cgi/content/full/291/5510/1952/DC1.
16. The Ain Settara section (STW) is ~50 km south of the El Kef section. The thickness of the K-T clay in the two sections is approximately equal, and the STW section has been correlated to the El Kef stratotype (J. Kirschvink, personal communication) (17).
17. C. Dupuis, E. Steurbaut, M. F. Matmati, abstracts presented at the International Workshop on Cretaceous-Tertiary Transition, Tunis, Tunisia, 13 to 16 May 1998.
18. S. Mukhopadhyay, K. A. Farley, A. Montanari, *Geochim. Cosmochim. Acta* **65**, 653 (2001).
19. K. A. Farley, in *Accretion of Extraterrestrial Matter Throughout Earth's History*, B. Peucker-Ehrenbrink, B. Schmitz, Eds. (Kluwer, Dordrecht, Netherlands, in press).
20. A. O. Nier, D. J. Schlutter, *Meteoritics* **25**, 263 (1990).
21. D. B. Patterson, K. A. Farley, M. D. Norman, *Geochim. Cosmochim. Acta* **63**, 615, (1999).
22. K. A. Farley, A. Montanari, E. M. Shoemaker, C. S. Shoemaker, *Science* **280**, 1250 (1998).
23. M. V. Sykes, A. A. Lebofsky, D. M. Hunter, F. L. Low, *Science* **232**, 1115 (1986).
24. P. R. Weissman, *Ann. N.Y. Acad. Sci.* **822**, 67 (1997).
25. S. J. Kortenkamp, S. F. Dermott, *Science* **280**, 874 (1998).
26. At STW, He measurements were made from the Ir-rich layer (17), and 20 and 80 mm above this layer (Table 1). On the basis of the three measurements, we assign an average ^{3}He of $20 \times 10^{-15} \text{ cm}^3$ standard temperature and pressure (STP) g^{-1} for the boundary clay. $^3\text{He}/^4\text{He}$ ratios at STW (Table 2) are close to typical crustal ratios of 0.03 R_x (19), suggesting that 20% or less of ^{3}He is extraterrestrial. A reasonable lower limit of the crustal end-member is 0.015 R_x (19), and we adopted this value for calculating $^{3}\text{He}_{\text{Et}}$. Hence, the computed duration of the boundary event from STW is an upper limit.
27. J. Smit, *Annu. Rev. Earth Planet. Sci.* **27**, 75 (1999).
28. L. Becker, R. J. Poreda, T. E. Bunch, *Proc. Natl. Acad. Sci. U.S.A.* **97**, 2979 (2000).
29. The total ^3He contribution from the bolide in the Italian K-T clay cannot exceed the ^3He concentration of $15 \times 10^{-15} \text{ cm}^3 \text{ STP g}^{-1}$ in the fallout lamina at STW, which is <8% of the measured ^3He in the Italian K-T clays.
30. K. J. Hsu, J. A. McKenzie, Q. X. He, *Geol. Soc. Am. Spec. Pap.* **190**, 317 (1982).
31. S. D'Hondt, P. Donaghay, J. C. Zachos, D. Luttenberg, M. Lindinger, *Science* **282**, 276 (1998).
32. J. Smit, *Geol. Mijnbouw* **69**, 187 (1990).
33. S. C. Cande, D. V. Kent, *J. Geophys. Res.*, **100**, 6093 (1995).
34. We thank J. Kirschvink and T. Raub for providing the STW samples (sample collection funded by NSF EAR9807741) and F. Robaszynski for discussion on the STW section. Funded by NASA and the David and Lucille Packard Foundation.

16 November 2000; accepted 1 February 2001

¹Department of Geological Sciences, University of Oregon, Eugene, OR 97403–1272, USA. ²Department of Geological Sciences, Brown University, Providence, RI 02912–1846, USA. ³Department of Geology and Geophysics, Woods Hole Oceanographic Institute, Woods Hole, MA 02543, USA. ⁴School of Oceanography, University of Washington, Seattle, WA 98195–7940, USA.

*To whom correspondence should be addressed at Brown University. E-mail: Robert_Allen_Dunn@brown.edu